JGR Oceans

RESEARCH ARTICLE
10.1029/2018JC014482

Retention and Leakage of Water by Mesoscale Eddies in the East Australian Current System

Paulina Cetina-Heredia[1,2], Moninya Roughan[1], Erik van Sebille[3], Shane Keating[1], and Gary B. Brassington[4]

[1]School of Mathematics and Statistics, University of New South Wales, Sydney, New South Wales, Australia, [2]Climate Change Research Centre, University of New South Wales, Sydney, New South Wales, Australia, [3]Institute of Marine and Atmospheric Research, Utrecht University, Utrecht, Netherlands, [4]Science and Innovation Group, Bureau of Meteorology, Sydney, New South Wales, Australia

Key Points:
- Median retention times are similar for cyclonic/anticyclonic eddies (24/27 days) but vary with geographic location
- Water in a region within the eddy close to uniform rotation is retained longer
- Water exchange relates to changes in eddy shape rather than size: increasing eccentricity leads to leakage while decrease promotes retention

Supporting Information:
- Supporting Information S1
- Figure S1

Correspondence to:
P. Cetina-Heredia,
p.cetinaheredia@unsw.edu.au

Citation:
Cetina-Heredia, P., Roughan, M., van Sebille, E., Keating, S., & Brassington, G. B. (2019). Retention and leakage of water by mesoscale eddies in the East Australian Current system. *Journal of Geophysical Research: Oceans*, *124*. https://doi.org/10.1029/2018JC014482

Received 16 AUG 2018
Accepted 18 MAR 2019
Accepted article online 21 MAR 2019

Abstract Mesoscale eddies are ubiquitous in the ocean, transporting semi-isolated water masses as well as advecting tracers and biota. The extent to which eddies impact the environment depends on the time they retain water parcels. Here we quantify retention times of mesoscale eddies in a (1/10)° model of the East Australian Current and its extension along the southeast coast of Australia. We find that retention times vary widely, between 3 and 357 days, but peak around 24 and 27 days for anticyclones and cyclones, respectively. Changes in eddy shape, though not in eddy size, relate to water exchange between the eddy and the background flow. An increase in eccentricity (eddy elongation) often leads to water leakage, while a decrease is associated with water retention. Thus, the change in eddy eccentricity can be used as a diagnostic of the eddy's likelihood to exchange water with its surrounding. We find that water within a region of the eddy that is close to uniform rotation and rotating faster than uniform vorticity is more likely to be retained. Typical retention times are long enough for eddies to transport water across regions of contrasting hydrographic properties, develop a biogeochemical response, and influence connectivity patterns.

Plain Language Summary Eddies occur globally throughout the ocean carrying water, its properties, and biota. This study quantifies the time that eddies along southeast Australia retain water elucidating their potential to affect the environment, for instance, by transporting warm East Australian Current water poleward, or the larvae of marine organisms. Our results show that eddies typically retain water over a month irrespective of their direction of rotation; however, the time they retain water varies with geographical location. Water is retained for longer in anticyclonic eddies (rotating right) that distribute along the continental shelf break and in cyclonic eddies (rotating left) that occur offshore in the Tasman Sea. We also find that eddies that elongate tend to leak water while eddies that become more circular promote the retention of water. Our results suggest that eddies along southeast Australia are likely to affect marine ecosystems.

1. Introduction

Eddies or isolated vortices are ubiquitous features in the ocean, influencing water mass transport and properties. For example, Agulhas rings can carry water masses across the entire South Atlantic influencing the transport of heat and salt (Beron-Vera et al., 2013; de Ruijter et al., 1999). In some regions eddy-induced zonal mass transport is comparable in magnitude to that of the wind and thermohaline-driven circulation (Zhang et al., 2014). Eddies also influence the oceans biogeochemistry modulating chlorophyll distribution by horizontal advection (Chelton, Gaube, et al., 2011) and inducing bursts of productivity through mechanical uplift of nutrient rich water (Bakun, 2006; Falkowski et al., 1991). Indeed, Benitez-Nelson et al. (2007) observed an eddy enhancing productivity and biomass in an otherwise oligotrophic ecosystem off the Hawaiian Islands. By trapping and recirculating water masses, eddies also transport and shape the pathways of particulates (inert or biota). Brach et al. (2018) show mesoscale eddies trapping and concentrating plastic litter in the North Atlantic with potential to transport it. Similarly, Lindo-Atichati et al. (2013) show that eddies in the Gulf of Mexico affect the distribution of fish larvae; moreover, the influence of eddies on connectivity (e.g., exchange of larvae among settlement habitats) is key in regions with swift currents (Cetina-Heredia et al., 2015; Yeung et al., 2001).

©2019. American Geophysical Union. All Rights Reserved.

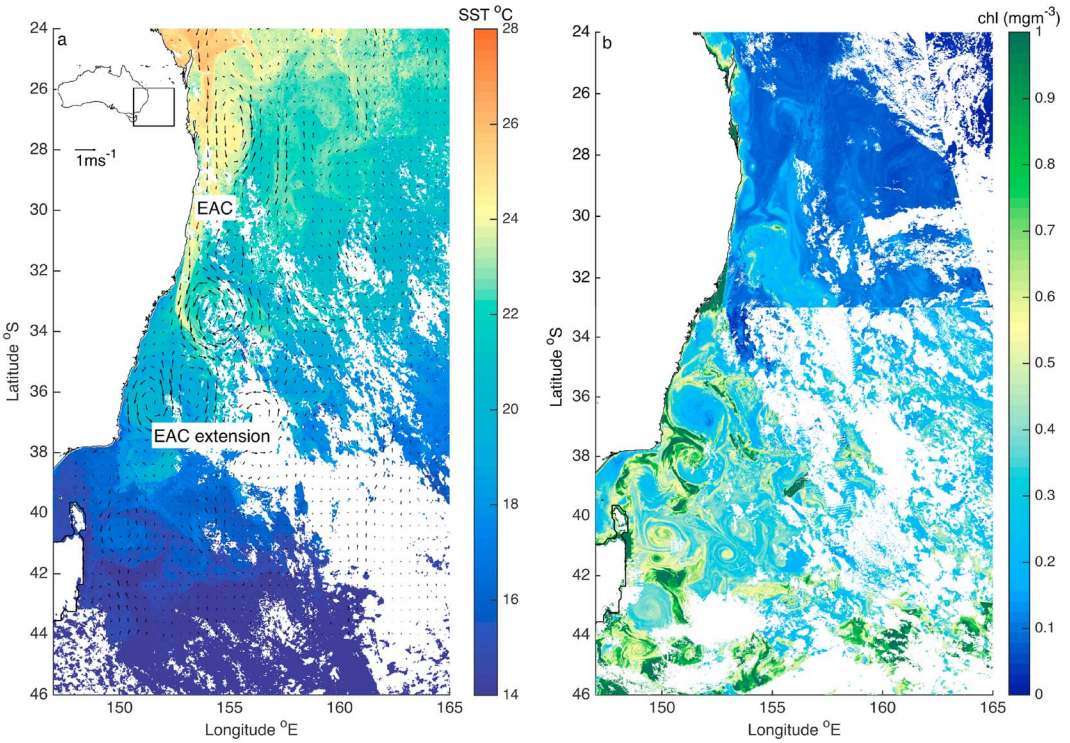

Figure 1. Snapshots of remotely sensed (a) sea surface temperature and geostrophic velocities (Advanced Very High Resolution Radiometer AVHRR L3S product) and (b) ocean color (Moderate Resolution Imaging Spectroradiometer MODIS) showing the presence of mesoscale eddies influencing temperature and chlorophyll distributions along southeast Australia on 26–27 November 2006. EAC = East Australian Current.

Eddy lifespan has been examined worldwide (e.g., Chaigneau et al., 2008; Chelton, Schlax, & Samelson, 2011; Lin et al., 2015; Pilo, Mata, & Azevedo, 2015), but only a handful of studies have quantified the time that eddies retain water parcels (e.g., Condie & Condie, 2016; d'Ovidio et al., 2013). Throughout their lifespan, eddies generally stretch and undergo filamentation causing dispersion of the fluid mass (Beron-Vera et al., 2013; Haller & Beron-Vera, 2013); thus, the potential of eddies to affect their environment through the retention and transport of water is not well known. Theoretical and modeling studies have examined the dynamics of retention and leakage by eddies (e.g., de Steur & van Leeuwen, 2004; Early et al., 2011; Froyland et al., 2015; Haller, 2005), and a few studies have identified water mass transport based on Lagrangian eddy boundaries (Beron-Vera et al., 2008, 2013; Wang et al., 2015). However, a systematic characterization of retention by mesoscale eddies has rarely been attempted (but see Abernathey & Haller, 2018). This study aims first to characterize eddies and retention time along southeast Australia and second to relate these eddy characteristics with instances of water entrainment, retention, or leakage.

Along southeast Australia, the circulation is dominated by the poleward flowing East Australian Current (EAC), the EAC extension, and mesoscale eddies (e.g., Ridgway & Dunn, 2003; Figure 1). Patterns of connectivity (Roughan et al., 2011), productivity (Roughan et al., 2017), and larval supply to the continental platform (Cetina-Heredia et al., 2019) in this region have been shown to be influenced by mesoscale eddies. Cetina-Heredia et al. (2014) showed that the contribution to poleward transport by eddies has increased in the last decade; moreover, eddies are projected to become more stable under a climate change scenario (A1B, Matear et al., 2013; Oliver et al., 2015). Some of the mesoscale eddy characteristics along southeast Australia have been identified; for instance, Pilo, Oke, et al. (2015) used altimetry to map their distribution and propagation and quantify their size, amplitude, and vorticity; Everett et al. (2012) quantified their biophysical properties; and Rykova and Oke (2015), Rykova et al. (2017) explored their hydrographic properties (temperature and salinity). Here we quantify their retention time. In addition, we explore if, and how, eddy metrics relate to retention.

A better understanding of the relation between eddy characteristics and water retention or leakage can aid predictions in terms of eddy retention times and the consequent impact on the environment. Here we

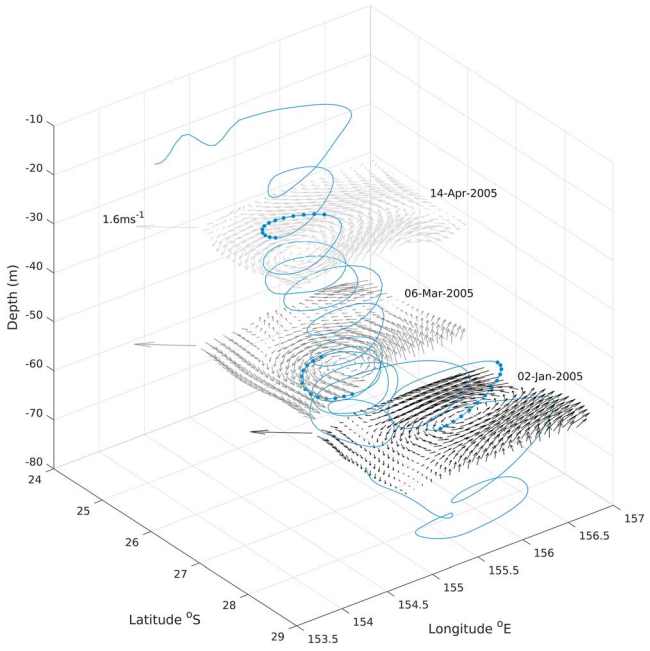

Figure 2. Three-dimensional trajectory of a particle (blue line) superimposed are examples of 2-D velocity fields used at three different time steps to characterize the eddy. The dots represent the particle positions every 6 hr that correspond to each 2-D velocity field analyzed (available every 3 days).

quantify that the time water parcels are retained within eddies and focus on metrics that characterize the eddy (e.g., diameter and vorticity) and on dynamical metrics that have been suggested to drive retention or leakage (e.g., degree of uniform rotation). Eddy metrics (e.g., diameter and vorticity) and retention diagnostics (e.g., degree of uniform vorticity and eccentricity) are averaged over the time period that water parcels are retained, and these metrics are then used to explore the relation with retention time. In addition, we use composites of eddy metrics across instances when water parcels are entrained, retained, and leaked.

In order to characterize eddies and their potential to retain water parcels, our approach combines Lagrangian and Eulerian techniques; first, we examine particle trajectories and their spin parameter (Ω_S, rotation) to quantify retention time from instances when water parcels enter, remain, and leave eddies; second, to verify the spin parameter diagnoses water parcels inside eddies, we corroborate the presence of eddies in velocity fields simultaneous to times when the spin parameter indicates looping trajectories; finally, we use these velocity fields to characterize the eddies (Figures 2 and 3).

1.1. Advantages of a Lagrangian-Eulerian Approach

Using a combined Lagrangian-Eulerian approach is convenient because identifying looping trajectories provides the means to quantify the time that diagnosed eddies retain water parcels. We implement a Lagrangian approach that does not focus on the eddy's lifespan, which is one of the characteristics derived from Eulerian eddy detection and tracking methods. Using the time a water parcel is trapped within an eddy instead of its lifespan is important because an eddy may persist after leaking water; thus, the eddy lifespan is not necessarily representative of the retention time. On the other hand, motivated by drifter observations, Lagrangian techniques to estimate eddy characteristics (e.g., size and vorticity) from looping trajectories have been developed (e.g., Brassington,

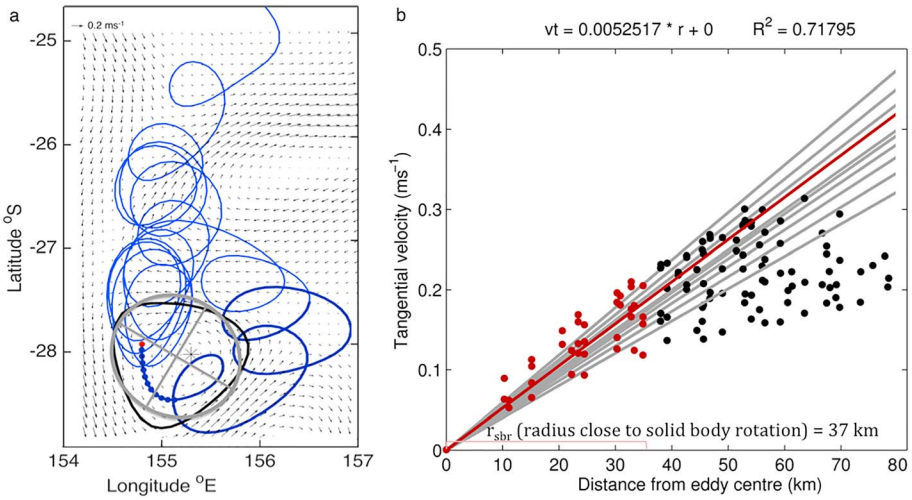

Figure 3. (a) Trajectory of a particle while entrained in an eddy (blue line) superimposed on the velocity field (63 m deep) corresponding to the first 3 days of the particle trajectory (positions indicated by the red—start—and subsequent blue dots); the darker blue indicates 30 days of the trajectory. The black asterisk and contour represent the identified eddy center and edge, the gray contour shows the fitted ellipse, and the gray lines show the semimajor and semiminor axes of the ellipse. (b) Linear regressions of tangential velocity as a function of distance from the eddy center; each line represents a regression starting by fitting a line to data within one grid cell from the eddy center, followed by using the data within two grid cells from the eddy center and so forth until including all data points within the eddy. The eddy uniform vorticity (Ω_u) is the slope of the line associated with the best goodness of fit (red line).

2010; d'Ovidio et al., 2013; Lilly et al., 2011); however, it is unclear how representative the information extracted from a single trajectory is.

An Eulerian approach based on velocity fields is therefore chosen for the characterization of eddies. Importantly, looping trajectories can be the consequence of inertial oscillations or Rossby waves (Flierl, 1981); although the inertial frequency in the region would cause looping trajectories over shorter time periods than those explored here (i.e., ~1 day), complementing eddy diagnosis from looping trajectories with an Eulerian observing framework is still necessary to verify that such trajectories are induced by an eddy rather than Rossby waves (Brassington et al., 2011). Finally, because Eulerian frameworks are often more comprehensive in space and time than Lagrangian when observing or estimating velocity fields, our Eulerian eddy characterization can be compared broadly; for instance, satellite altimetry provides fields of geostrophic velocities around the globe; thus, our findings can be easily related to mesoscale eddies elsewhere.

2. Methods

2.1. Data

We make use of a data set of particle trajectories, and associated Ω_S, described in Cetina-Heredia et al. (2014). The data set was generated using 3-D velocity fields from the Ocean Forecast for the Earth Simulator (OFES) and the Connectivity Modeling System (Paris et al., 2013), a Lagrangian tracking model. OFES is an eddy-resolving model with (1/10)° horizontal spatial resolution and 54 vertical layers (Masumoto et al., 2004); it compares well with observations in the study region (van Sebille et al., 2012) and has been used to quantify long-term (from 1980 to 2010) transport by the EAC, its extension, and eddies (Cetina-Heredia et al., 2014). The model is initialized with temperature and salinity fields from the World Ocean Atlas and forced with National Centers for Environmental Prediction from 1950 to 2007 (Masumoto et al., 2004).

The Cetina-Heredia et al. (2014) data set was constructed from simulated trajectories of particles released in a spatial pattern that tags the EAC every third day (temporal resolution of OFES outputs) from 1980 to 2010, specifically seeded along a latitudinal section at 28°S where the EAC is coherent, throughout the water column, and at grid cells through which 95% of the instantaneous 3-D cumulative poleward transport occurs. The poleward transport was diagnosed with OFES velocity fields, and the number of grid cells or particles released every third day varied between 200 and 300 yielding a total of 34,324 in a year. The Lagrangian simulations rely upon the 3-D velocity fields and were run off-line with an integration time of 6 hr; the 3-D particle positions were also recorded every 6 hr. As the OFES velocity fields are only available every 3 days, Connectivity Modeling System uses tricubic interpolation of the velocity fields and particles' positions every 6 hr within the 3-day time step.

Here we used trajectories of particles released in 2005–2006. We determined that 500 trajectories were sufficient to sample mesoscale eddies in OFES model output ((1/10)° spatial resolution). The smallest eddies resolved by OFES are approximately 25 km in radius or 2.2 grid points. An eddy with this radius would cover an area of ~15 grid points. In order to detect this feature, a trajectory must enter these 15 grid points. Based on mean eddy kinetic energy, the region where eddies are likely to occur (i.e., where the mean EKE is equivalent or larger to 0.5 m^2/s^2, Figure 4) encompasses ~6,784 OFES grid points; thus, 453 trajectories would suffice to detect features spanning 13 grid points, assuming that the sampling is homogeneous and the eddies extend vertically in the water column. We randomly drew 500 trajectories from the 2005–2006 data to detect and diagnose mesoscale eddies. A top view and vertical distribution of the trajectories that entered eddies and were further analyzed are shown in Figure S1 in the supporting information.

2.2. Spin Parameter and Velocity Fields

Lagrangian stochastic models describe the motion of passive tracer particles in a turbulent flow using stochastic differential equations (Veneziani, Griffa, Reynolds, et al., 2005). Veneziani et al. (2004) applied the spin parameter (Ω_S) as one such Lagrangian stochastic model in the northwestern Atlantic Ocean and showed it effectively parameterizes the main statistical properties of the mesoscale turbulence by identifying looping and nonlooping regimes. The spin parameter describes the mean rotation per time interval computed along a particle trajectory (Griffa et al., 2008); it represents a good estimate of the relative vorticity of the vortex core in which the loopers are embedded and it follows the vortex temporal evolution

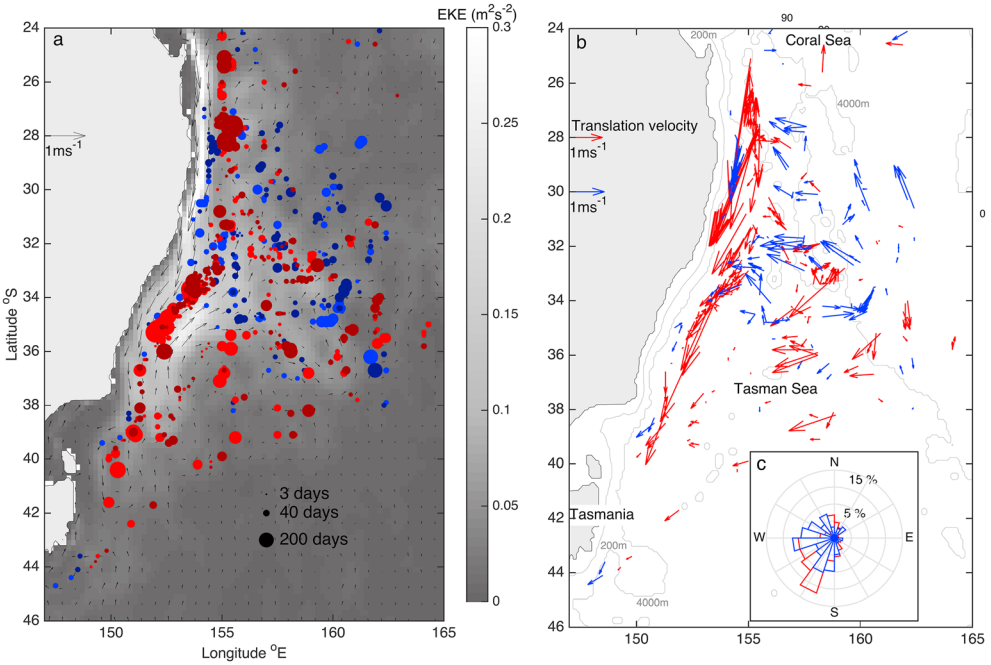

Figure 4. (a) The 2005–2006 mean eddy kinetic energy (EKE), mean geostrophic velocities capturing the (East Australian Current [EAC], EAC extension, and Tasman Front), and distribution of anticyclonic (red) and cyclonic (blue) eddies at the moment water parcels are entrained (dark tone) or leaked (light tone). The size of the symbol is scaled with retention time; arrows represent the mean geostrophic velocity from 2005 to 2006. (b) Translation velocities for anticyclones (red) and cyclones (blue); gray lines show the 200- and 4,000-m bathymetry contours. (c) Rose of translation direction of anticyclonic (red) and cyclonic (blue) eddies; numbers indicate the percentage of eddies (anticylones and cyclones separately) moving in each direction bin without considering those that do not move.

(Veneziani, Griffa, Garraffo, et al., 2005). Cetina-Heredia et al. (2014) used the spin parameter to diagnose the contribution to poleward transport of EAC eddies. Here we extend this work to investigate the kinematics of the eddies themselves; we use the spin parameter Ω_S to distinguish between looping and nonlooping Lagrangian particle trajectories, determine the direction and magnitude of rotation in the looping, and identify instances when particles were inside eddies as well as the time they remained inside the eddy. The expression for the spin parameter is

$$\Omega_s = \frac{\left\langle u' \mathrm{d}v' - v' \mathrm{d}u' \right\rangle}{\mathrm{EKE}\ 2\Delta t} \tag{1}$$

where u' and v' are the east-west and north-south Lagrangian velocity anomalies, respectively, with $u = \overline{u} + u'$ and $v = \overline{v} + v'$ being a decomposition of the east-west and north-south velocity fields into the time mean (over 30 years) and time-varying component within each (1/10)° by (1/10)° grid cell, respectively, $\mathrm{d}u'$ and $\mathrm{d}v'$ are the time differentials of the east-west and north-south Lagrangian velocities, respectively, Δt is the time step used to record particle position (6 hr), $\langle\rangle$ represents an average of values over 30 days of a particle trajectory, and EKE is the eddy kinetic energy given by

$$\mathrm{EKE} = 0.5\left\langle u'^2 + v'^2 \right\rangle \tag{2}$$

The Lagrangian velocities are computed from particle trajectories; further details to calculate the spin parameter are described in Cetina-Heredia et al. (2014). Each particle trajectory is associated with a spin parameter value every 30 days; threshold values of $\Omega_S > 0.2\ \mathrm{day}^{-1}$ and $\Omega_S < -0.2\ \mathrm{day}^{-1}$ were applied to identify if each 30-day segment of all particle trajectories was rotating anticyclonic or cyclonically, respectively (i.e., inside an eddy). Van Sebille et al. (2012) find that spin parameter threshold values between 0.15 and 0.3 day^{-1} recognize eddies in the Tasman Sea, and Cetina-Heredia et al. (2014) show that 0.2 day^{-1} is an accurate

value to discriminate between looping and not looping trajectories. Thus, a spin parameter of 0.2 day^{-1} diagnoses eddies in the region.

The first step was to identify instances when a particle entered an eddy; thus, in our approach the sample unit is a particle trajectory. Once an eddy is detected using Lagrangian data, other eddy properties (such as eddy radius or rotation period) can be diagnosed using Eulerian methods. These methods are typically based on physical metrics derived from the velocity fields (e.g., the Okubo-Weiss parameter), or on the geometry of the velocity fields (Chaigneau et al., 2008; Sadarjoen et al., 1998). Both type of methods have been applied to examine mesoscale eddies (e.g., Chelton et al., 2007; Chelton, Schlax, & Samelson 2011; Chaigneau et al., 2008; Nencioli et al., 2010). The use of the Okubo-Weiss parameter, which contrasts vorticity and strain, requires the choice of a threshold value to identify the edge of the eddy; in contrast, methods based on flow geometry use closed contours of the stream function around an identified eddy center. Here we opt for a method based on flow geometry to minimize sensitivity to the choice of a threshold value for a dynamical parameter (i.e., Okubo-Weiss) as well as the uncertainty associated with the introduction of noise when computing vorticity and strain from velocity derivatives.

The method we use to diagnose eddy properties is described in Nencioli et al. (2010). The method identifies an eddy center when four constraints are satisfied: The velocity vector changes sign in the zonal and meridional directions when crossing the center, the velocity magnitude has a local minimum around the eddy center, and the direction of velocity vectors needs to change with a constant sense of direction. Once the eddy center has been identified, eddy characteristics, such as radius or rotation period, can be diagnosed. The skill of the Nencioli et al. (2010) method in terms of accuracy detecting true eddies satisfies criteria for acceptable performance by automated algorithms (e.g., above 80% success of detection rate, Chaigneau et al., 2008) and outperforms that of the Okubo-Weiss parameter (Nencioli et al., 2010). This method has been used to explore eddy characteristics over regional and ocean basin scales (Dong et al., 2012; Liu et al., 2011).

To implement the method, two parameters need to be specified: parameter a, which indicates over how many grid points from the center an increase in velocity should occur, and parameter b, which determines the number of grid points to define the local minimum velocity. We use $a = 4$ and $b = 3$; with OFES's spatial resolution ((1/10)°, within our domain that is 7.4–10.1 km in the zonal and 11.1 km in the meridional direction), this implies that rotation and an increase in velocity moving away from the center have to occur within at least 29–44 km of the center to identify an eddy. Although the spatial resolution varies in the zonal and meridional directions, because we use the spin parameter to identify eddies and the Nencioli et al. (2010) method to diagnose eddy characteristics, the choice of parameters a and b is not crucial in terms of eddy detection; once an eddy is detected, the characterization (e.g., eddy radius estimate) is not sensitive to parameter choice.

2.3. Retention Time

The retention time for each particle is equivalent to the time period during which the particle has $|\Omega_S| > 0.2$ day^{-1}, while this is a first Lagrangian diagnostic, the retention time is corroborated by conjunct examination of the particle position and eddy boundaries identified from velocity fields (Eulerian diagnostic); thus, retention times satisfy both a $|\Omega_S| > 0.2$ day^{-1} for the particle trajectory and a particle position within the eddy boundaries thereby benefitting from both a Lagrangian and Eulerian perspective. Previous studies have shown that a 0.2-day^{-1} value diagnoses eddies in the region accurately (Cetina-Heredia et al., 2014) and is therefore suitable to quantify retention time by eddies. Each time a particle loops ($|\Omega_S| > 0.2$ day^{-1}) we identify the eddy from the associated velocity fields (Figure 3) until the particle leaves the eddy ($|\Omega_S| < 0.2$ day^{-1}). Each time step OFES velocity fields are available (3 days) the particle's vertical position is used to determine the depth of the velocity field used to characterize the eddy (Figure 2). Additionally, the depth extent of the eddy is also diagnosed applying the Nencioli algorithm on 2-D velocity fields at depths above and below that of the particle's position; this analysis restricted detection to eddies with the same center position as that identified at the particle's depth; thus, it only identifies the depth extent over which the eddy is straight. The eddy characteristics are associated with the time the particle remains inside the eddy (retention time Rt). We examine how retention diagnostics relate to the time water parcels remain inside eddies, and differences in retention diagnostics across eddies that entrain, retain, or leak particles. Cyclones and anticylones are analyzed separately.

2.4. Eddy Characterization and Retention Diagnostics

We chose a set of variables that characterize the eddy and its dynamics: the eddy radius (r), vorticity (Ω), period (T), and Rossby number (Ro). Similarly, we estimated metrics that may relate to the eddy's potential to retain water parcels: the region within the eddy that is close to solid body rotation (referred to as solid body rotation radius r_s) and the ratio of the eddy rotation velocity to the velocity at which the eddy is translated over the background flow (Uc), eddy eccentricity (e), and tendency in eccentricity over time (de/dt). All metrics are computed for every time step (3 days) during the time a particle remains inside an eddy; the average over such time period of each property is used to represent each eddy and to relate these metrics with retention time.

2.4.1. Eddy Characteristics: Radius, Vorticity, Period, and Rossby Number

The eddy radius (r) is determined as the mean distance between the eddy center and the outermost closed streamline across which the radial velocity is still increasing (Nencioli et al., 2010). The eddy vorticity (Ω) is estimated by fitting a straight line to data points determined by the distance from the eddy center and the tangential velocity (v_t); thus, the eddy vorticity is the slope of the linear fit $v_t = \Omega r$. The eddy period (T) is given by $T = 2\pi/\Omega$. Finally, the Rossby number is defined as the vorticity normalized by the absolute Coriolis parameter at the eddy center, $Ro = \Omega/|f|$.

2.4.2. Retention Diagnostics

2.4.2.1. Solid Body Rotation and Rotational to Translation Velocity Ratio

Uniform or solid body rotation implies that a water parcel rotates at a tangential velocity (v_t) that increases linearly as it is further from the eddy center. In the ocean, interaction with the background flow prevents uniform rotation or uniform rotation throughout the eddy extent; Early et al. (2011) propose that only an inner core of the eddy delimited by the zero relative vorticity contour retains water parcels, while an outer region exchanges water with its surrounding; thus, for each eddy we diagnose a region close to solid body rotation (radius r_s). This region is identified by fitting a straight line to data points determined by the distance from the eddy center against tangential velocities obtained from the Eulerian velocity fields. We use velocity data from grid cells between the eddy center and the eddy edge. The fit and goodness of fit is first obtained including data within a grid cell from the eddy center; second, including data within two grid cells from the eddy center; and so forth until all data between the center and eddy edge are included. The radius of solid body rotation is that when the inclusion of more data points for the fit does not give a better goodness of fit (R^2, Figure 3b). The slope for the best fit is recorded as the eddy uniform vorticity (Ω_u). The radius of solid body rotation, uniform vorticity, and goodness of fit is obtained for every time step during the time a particle is inside an eddy, and the averages are used to relate these metrics with retention time.

In addition, we define U_c as the ratio of rotational to translation velocity; because we are interested in a metric that reflects the potential to retain a water parcel and because retention time corresponds to the time a particle remains inside an eddy, the rotational velocity used to compute U_c is the tangential velocity at the location of the particle (v_{tp}). The translation velocity is computed from the displacement of the eddy center in time as $v_{tp} = dr_{ec}/dt$, where dr_{ec} is the distance between eddy centers in a time step dt.

2.4.2.2. Eccentricity and Eccentricity Change

The least squares method is used to fit an ellipse to the data points determined by the longitude and latitude defining the edge of the eddy without constraining the eddy center. Eccentricity is then calculated as $e = \sqrt{1-\frac{e_b^2}{e_a^2}}$, where e_a and e_b are the semimajor and semiminor axis of the ellipse, respectively (Figure 3). A value of 0 implies an isotropic eddy with circular shape and axes of same magnitude, while a value close to 1 implies an anisotropic eddy with an elongated elliptical shape where one axis is considerably larger than the other. Finally, the change in eccentricity over time is computed as a measure of changes in shape of the eddy, and whether it is becoming more (+) or less (−) elongated.

3. Results

3.1. Eddy's Spatial Distribution, Retention, and Translation

We use particles seeded in 2005–2006 that displayed looping trajectories examining 255 and 130 instances when particles entered anticyclonic and cyclonic eddies, respectively.

Table 1
Percentage of Anticyclonic and Cyclonic Eddies Translated in Each Direction and Corresponding Median and Interquartile (25%–75%) Translation Velocities

	Anticyclones			Cyclones		
Direction	%	Median (m/s)	Interquartile range (m/s)	%	Median (m/s)	Interquartile range (m/s)
East	2.7	0.3	0.16–0.53	3	0.5	0.40–0.73
NE	4.3	0.3	0.20–0.40	6.9	0.2	0.12–0.34
North	11.4	0.3	0.19–0.80	6.9	0.3	0.16–0.43
NW	5.5	0.4	0.14–0.44	15.4	0.5	0.20–0.94
West	16.1	0.3	0.13–0.49	24.6	0.3	0.17–0.79
SW	32.5	0.4	0.15–0.81	18.5	0.3	0.25–0.54
South	13.7	0.2	0.13–0.64	15.4	0.3	0.14–0.69
SE	5.9	0.2	0.08–0.38	3.1	0.1	0.07–0.15
All directions	92.1	0.3	0.12–0.52	93.8	0.4	0.15–0.60
No translation	7.9			6.2		

Note. The direction of translation and translation velocities are computed considering the eddy translation since water entrainment until leakage.

The regions where we detect water parcel entrainment into and leakage out of mesoscale eddies (Figure 4) correspond to an area where sea surface height variability is large (Mata et al., 2006), and that has been associated with high eddy kinetic energy (Kerry et al., 2016; O'Kane et al., 2011; Schiller et al., 2008). Eddies are often aligned with the continental shelf break along the EAC and EAC extension, and over a quasi-zonal band into the Tasman Sea at ~31°S where the EAC separates frequently and gives rise to the Tasman Front (Figure 4). Anticyclonic eddies propagate most often in a southwestward direction (aligned with the shelf break) typically at speeds of 0.3 m/s. Conversely, cyclonic eddies generally move toward the west, including NW, SW, and west at speeds of 0.3 m/s, and a larger proportion is distributed throughout the Tasman Sea (Table 1 and Figure 4).

Retention times range from a few days to a year; the maximum retention time in the data here is ~75% longer in anticylones (maximum of 357 days) than in cyclones (maximum of 198 days); nevertheless, typical retention (i.e., interquartile range from the 25th to the 75th percentiles) by anticyclones is marginally shorter (12–45 days) than that by cyclones (18–51 days, Figure 5a). Interestingly, retention within anticyclones is consistently longer for eddies downstream of the latitude where the EAC typically separates (i.e., 32.4°S, Cetina-Heredia et al., 2014) and closer to the coast. In contrast, retention by cyclonic eddies is slightly larger offshore (Figure 4).

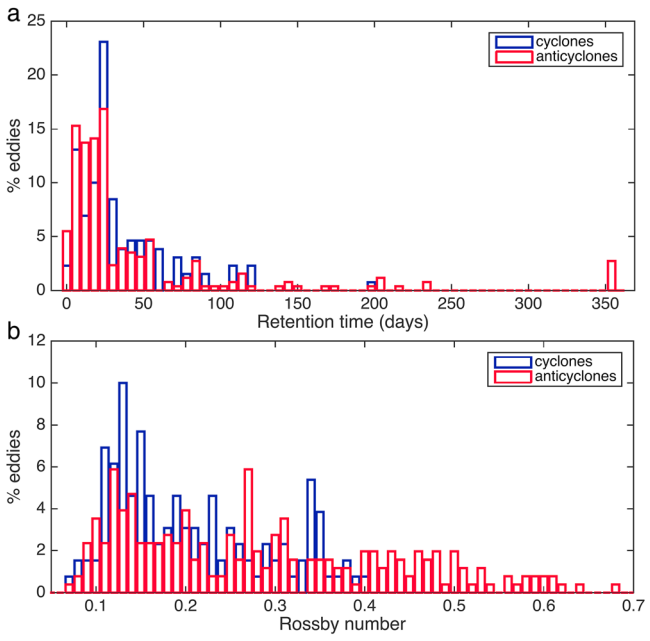

Figure 5. Frequency histogram (percent of eddies) of retention time (a) and Rossby numbers (b) for both anticyclonic (red) and cyclonic (blue) eddies.

3.2. General Eddy Characteristics: Radius, Vorticity, Period, and Rossby Number

Anticyclonic eddies vary in radius between 23 and 123 km and extend straight through the water column over ~450 m. Their vorticity ranges from 0.25×10^{-5} to 3.2×10^{-5} s^{-1} implying water parcels may take as little as 2 days or up to 29 days to complete an orbit around the eddy. Cyclonic eddies also have a similar depth extent and a large radius range but are marginally smaller than anticyclones, with radii between 25 and 94 km. Their vorticity is similar in magnitude to that of anticyclones but with a smaller range of 0.31×10^{-5} to 1.5×10^{-5} s^{-1}, resulting in water parcels orbiting the eddy in 5–23 days. Overall, anticyclones tend to be larger than cyclones and have higher vorticity/shorter period (Figures 6a and 6b). The frequency distributions of size and vorticity for mesoscale eddies are skewed toward smaller values; hence, there are more smaller eddies with low vorticity than large eddies with high vorticity.

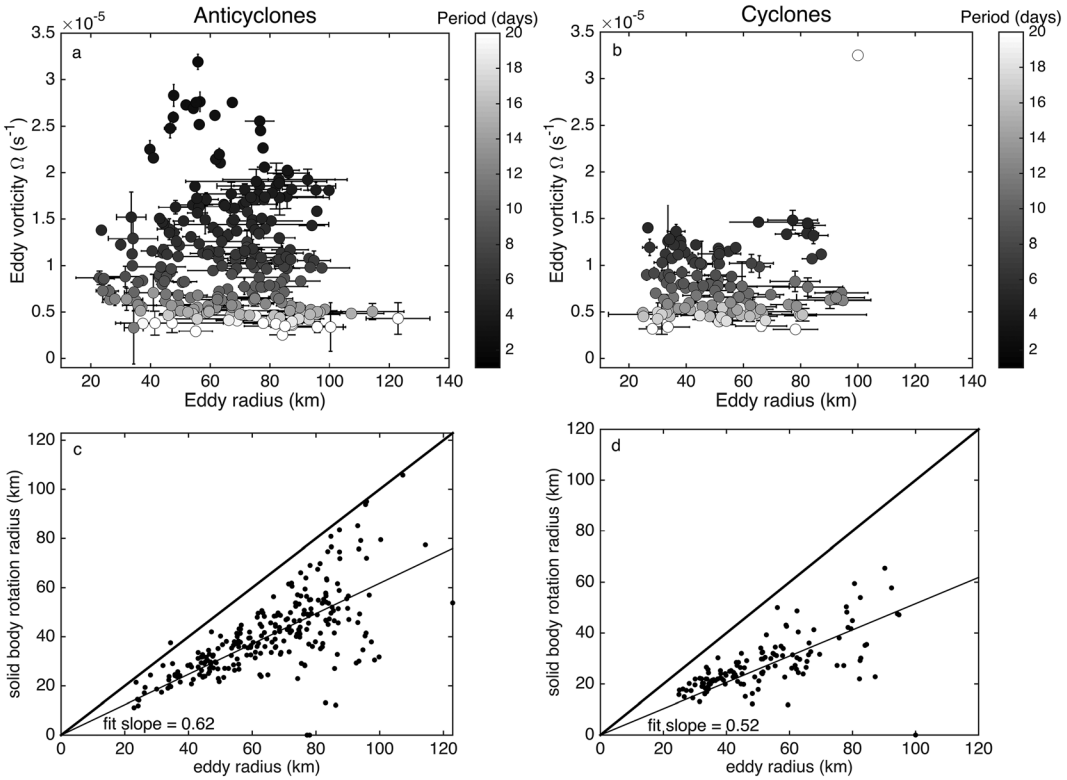

Figure 6. (a and b) Eddy radius and vorticity (mean ± standard error) for (a) anticyclones and (b) cyclones. Means and standard errors are computed over time, spanning the time period that a particle remains inside an eddy. (c and d) Eddy radius versus solid body rotation radius for (c) anticyclones and (d) cyclones. The linear fit and slope are shown with a thin line; the thick line represents the rotation radius equal to the eddy radius.

The radius of solid body rotation is always smaller than the radius of the diagnosed eddy edge. Thus, while median eddy radius reach 67 and 47 km for anticyclones and cyclones, respectively, median solid body rotation extend only within 38 and 25 km from the eddy center for anticyclones and cyclones, respectively; commonly, the radius of solid body rotation is ~50%–60% smaller than the eddy radius (Figures 6c and 6d).

Rossby numbers are significantly smaller than unity suggesting mesoscale eddies are predominantly in approximate geostrophic balance; specifically, we find Rossby numbers with a median (interquartile range) of 0.18 (0.13–0.26) and 0.26 (0.15–0.4) for cyclones and anticyclones, respectively (Figure 5b).

3.3. Eddy Retention Diagnostics

3.3.1. Solid Body Rotation

Comparison of the tangential velocity expected from the eddy uniform rotation and that at the location of the particle inside the eddy reveals most particles rotating faster or slower than uniform vorticity. Most of the particles within the region close to solid body rotation have the same or faster tangential velocities than that expected from uniform vorticity. More importantly, for both anticylones and cyclones, a significantly higher proportion of particles that show long retention times (e.g., retention time $\geq$ 100 days) lie inside the region close to solid body rotation and are associated with faster rotation than uniform vorticity, particularly for anticyclones (Figure 7). Conversely, particles whose mean location is outside the region close to solid body rotation are always rotating at a slower velocity than that expected for uniform vorticity and associated with shorter retention times (Figure 7). This is corroborated with an analysis of variance, which shows that for anticyclones and cyclones, retention times are significantly larger for particles within the region close to solid body rotation ($p \ll 0.01$); similarly, for anticyclones, those particles that rotate at a faster velocity than that expected from uniform vorticity are retained for longer ($p \ll 0.01$). Interestingly, we find that tangential velocities of particles inside anticyclones can be faster than those for cyclones and deviate further from tangential velocities expected from uniform vorticity (Figure 7); such particles also show the largest retention

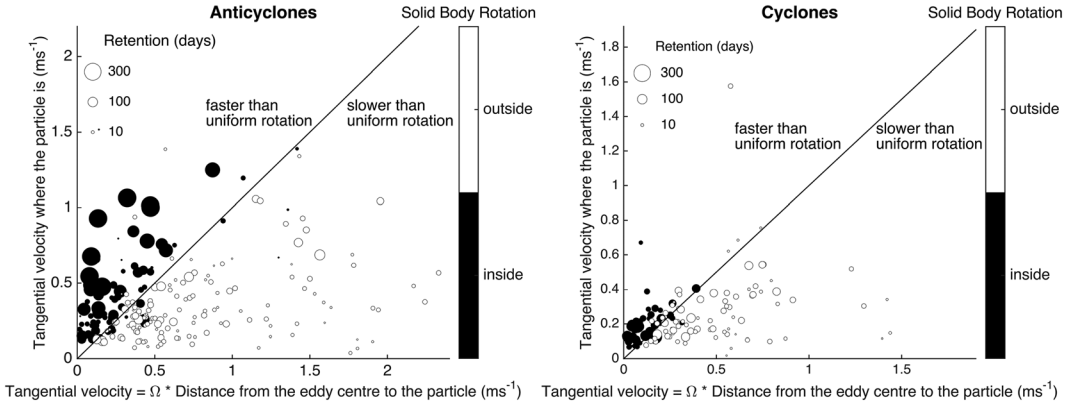

Figure 7. Tangential velocity at the particle location (v_{tp_u}) computed from uniform vorticity (Ω_u), against tangential velocity at the particle location (v_{tp}) from the Eulerian velocity field. The size of the symbol is scaled by retention time; black symbols show cases when the mean distance of the particle from the eddy center is within the region close to solid body rotation, and white symbols when it is outside.

times; this may be an indication of anticylonic eddies merging constructively as known to occur throughout the Pacific (Qiu-Yang et al., 2016) including off southeastern Australia.

3.3.2. Ratio of Rotational to Translation Velocity (U_c)

For an eddy to transport water, the ratio of the velocity of the rotational velocity to the eddy's translational velocity (U_c) has to be larger than unity (Early et al., 2011). In agreement, we find that longer retention occurs in eddies that have large U_c; for instance, particles that remain in eddies for longer than 30 days have U_c that are at least larger than 2. Similarly, the largest retention time is associated with the largest U_c. Nevertheless, there are instances when U_c is large and retention is short (Figure 8). Therefore, there are factors other than the balance between translation and eddy rotation influencing retention of water by eddies.

3.3.3. Eccentricity and Eccentricity Change

Vortex instability or the interaction of eddies with the background flow may cause differential rotation, changes in the eddy shape (e.g., change in eccentricity), and an opportunity for water exchange (de Steur & van Leeuwen, 2004). Our results show that changes in eccentricity are larger in magnitude across eddies that leak water parcels than for those that retain them. Moreover, the tendency of eccentricity across cyclonic and anticyclonic eddies that leak water parcels is positive, implying that the eddy is becoming more elongated (i.e., toward larger anisotropy). In contrast, changes in eccentricity when particles are retained are toward isotropy (Figure 9). Interestingly, there was no clear relation between water entrainment, leakage, or retention and changes in eddy size (increase or decrease of the area of fitted ellipses).

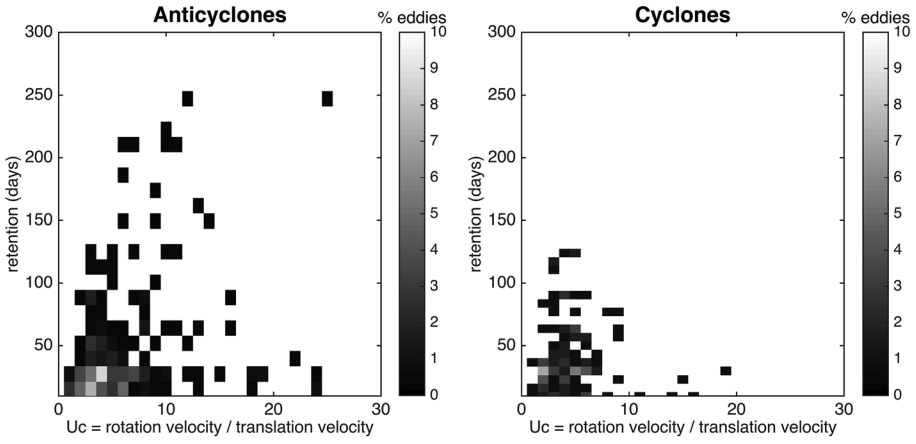

Figure 8. Frequency histogram (percent of eddies) for the ratio of eddy rotation velocity to eddy translation velocity (U_c), and retention time (days).

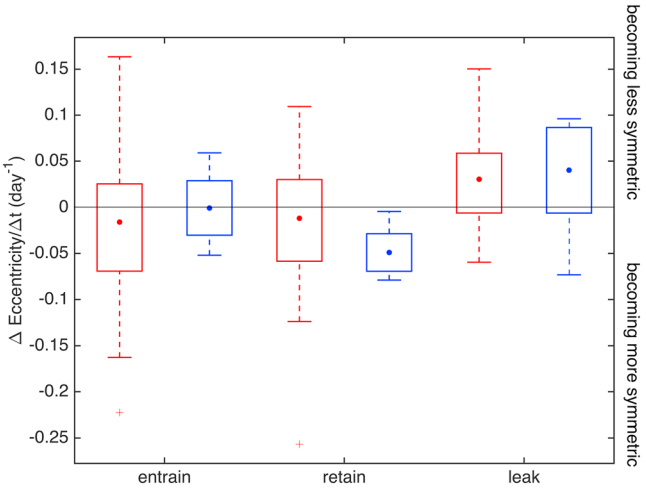

Figure 9. Tendency in eccentricity relative to the likelihood of water being entrained, retained or leaked. The bars extend from the 25th to the 75th percentiles, the dot indicates the mean, and the whiskers encompass the whole data range (red) anticyclones and (blue) cyclones.

4. Discussion

4.1. Summary of Retention Times, Eddy Characteristics, and Method Limitations

Based on mesoscale modeling outputs, we show that the retention by mesoscale eddies shed by the EAC or entraining EAC water varies significantly; eddies can retain water parcels over a year and can also leak easily and retain water only for a few days. The median retention time by eddies is close to a month (Figure 5a). Mesoscale eddies in the EAC system also have a wide range of sizes, vorticities, eccentricity, and shape fluctuations (i.e., changes in eccentricity with time). Eddy diameter varies over a factor of 5, roughly from 50 to 250 km. Depending on size and vorticity, a water parcel may take as little as 2 days and up to 29 days to complete an orbit around the eddy (Figures 6a and 6b). We find that anticyclones are typically larger than cyclones and can retain water parcels for longer, with median diameters of 135 and 94 km, and maximum retention times of 357 and 198 days for anticyclones and cyclones, respectively (Figure 5a). However, both the diameter and retention time ranges encompassing the 25th to the 75th percentiles are similar irrespective of the direction of rotation (Figure 5a). Nevertheless, we find differences in their spatial distribution; retention by anticyclonic eddies is consistently longer immediately downstream of typical EAC separation latitudes. Conversely, cyclones located offshore in the Tasman Sea retain water for longer than those close to the continent (Figure 4a). This suggests that anticyclones are likely to transport water poleward along the southeast coast of mainland Australia into the coastline of Tasmania, and subsequently toward the Southern Ocean (Pilo, Oke, et al., 2015), while cyclones are more likely to transport water within the Tasman Sea westward (from NW to SW).

Focusing on EAC eddies or eddies that entrain EAC water, we analyze trajectories of particles released outside eddies, across a latitudinal section where the EAC is most coherent (at 28°S). The time when particles enter an eddy might not coincide with the moment of eddy formation; therefore, retention time could be underestimated, for instance, for particles that first enter an eddy that is already decaying. Given the particle release location, particles entering eddies late in their lifespan may be more common for eddies that form in the Tasman Sea than for eddies formed along the EAC poleward path or shed by the EAC; hence, our results may be underestimating retention time by offshore eddies.

Because the EAC is known to shed anticyclonic eddies consistently (Bull et al., 2017; Cetina-Heredia et al., 2014), it is not surprising that there are more particle trajectories entering anticyclones than cyclones. Nevertheless, the largest proportion of particles entering anticyclones is also determined by the larger proportion of anticyclones relative to cyclones in the study region (Oliver et al., 2015; Pilo, Mata, & Azevedo, 2015).

Our estimates of retention and eddy characterization only account for mesoscale dynamics. According to Griffies and Treguier (2013), a model's effective resolution is 6–10 times its grid spacing; therefore, the model used in this study does not resolve features of spatial scales smaller than 44.4 km (6 times 7.4 km, i.e., the minimum grid spacing), which are relevant to nonlinearities that may influence properties such as vorticity.

4.2. How Do Eddy Characteristics, Retention Times, and Distribution in the EAC Compare to What Has Been Found in This and Other Regions?

The vorticity, radius, and distribution of mesoscale eddies diagnosed with weekly merged altimetry fields (Everett et al., 2015; Pilo, Mata, & Azevedo, 2015) are similar to those identified in our study. Individual mesoscale eddies in the region studied with models (Macdonald et al., 2016, Oke & Griffin, 2011) and more recently observed (Roughan et al., 2017) also lie within the realm of eddies presented here.

Regarding their spatial distribution, and also in agreement with our results, Pilo, Mata, and Azevedo (2015) found eddies over the entire Tasman Sea with higher density south of the EAC separation and clustered over the continental shelf break. The alignment of eddies with prevailing currents in the region (i.e., EAC, EAC extension, and Tasman Front) suggests that their formation is associated with current instabilities. In addition, Pilo, Mata, and Azevedo (2015) observed most of the EAC eddies propagating westward. Similar eddy's

distribution and movement are identified in this study and by Oliver et al. (2015) from modeled velocity fields of contemporary and future circulation (projection of a climate scenario); however, the latter shows an enhanced difference in the distribution of cyclones and anticyclones where cyclones are more common in the Tasman Sea and anticyclones along the coast. The prevalence of anticylones along the EAC extension and cyclones across the Tasman Sea is also evident in our results (Figure 4).

Few studies focus on the time that eddies retain water parcels. In contrast to our results, d'Ovidio et al. (2013) found very few eddies with retention times longer than a month in the Kerguelen region of the Indian Ocean, and most common retention times of a few days (<10 days). Although retention times of eddies shed by the Agulhas Current (a Western Boundary Current analogous to the EAC) are not reported, these eddies are known to last few years (e.g., Duncombe Rae, 1991) and have therefore the potential to retain particles for time periods as long as the maximum retention times found in this study for the EAC. Condie and Condie (2016) examined 12 eddies under different oceanic conditions, distributed globally, and reported retention times between 5 and 67 days. We find median retention times of similar order of magnitude (~1 month) and also considerably longer maximum retention time (close to a year). Studies of large stable eddies in the North Atlantic have also reported retention of yearlong time scales (e.g., Lehahn et al., 2007; The Ring Group, 1981); our study suggests that stable eddies retaining water for long time periods (up to a year) occur in southeast Australia. This study is based on a numerical simulation with a spatial resolution of (1/10)°. Submesoscale and small mesoscale features that are not resolved at this spatial resolution may modify the retention time; nevertheless, the median retention times we find are the same order of magnitude than those obtained from observations of two-dimensional current fields, specifically from drifter releases inside large and small eddies in the region (~163 and ~35 km in diameter, respectively, Roughan et al., 2017).

4.3. Relationship Between Retention Diagnostics and Water Retention

The eddies we examine are embedded within a dynamic mean flow, and among other mesoscale eddies with which they interact (Pilo et al., 2018). As a consequence, eddies are in constant change, and predictions of the time they retain water parcels from mean eddy characteristics (e.g., radius, vorticity, and depth extent) are not robust. The large variability of average metrics over the eddy lifespan or time it retains a water parcel masks possible relationships between retention and eddy characteristics. Nevertheless, our analyses show eddies that become more circular (i.e., close to an idealized geostrophic balance) retain water parcels, while those that elongate (likely undergoing interaction and disturbance to the geostrophic balance) tend to leak water parcels; this is in agreement with observed pathways of drifting buoys within an anticyclone, which were leaked during its decay (Brassington et al., 2011). Thus, a measure of changes in eddy shape (i.e., tendency in eccentricity) can be used to diagnose the likelihood of immediate water retention or leakage by the eddy. This characteristic can be computed in near real time from geostrophic velocities obtained from satellite altimetry considering that satellite-derived fields of geostrophic velocities are often constructed from observations at different times and have low spatial resolution, which do not resolve submesoscale and small mesoscale features (Chelton, Schlax, & Samelson, 2011). Less limited to low temporal resolution in observations are those provided by Doppler radiometers such as the proposed new Sea surface KInematics Multiscale monitoring (SKIM) mission (Ardhuin et al., 2018), or more locally and with higher spatial resolution (e.g., of 1.5 km and 10.4° in the radial and azimuthal directions) by high frequency radars (Archer et al., 2017; Mantovanelli et al., 2017; Schaeffer et al., 2017).

Not surprisingly, the metrics that show a relationship with retention time are dynamical (e.g., ratio between translation to rotational velocity) and not simply geometrical (i.e., eddy size). Indeed, studies that have explored retention by eddies have not found a clear relation to size (Condie & Condie, 2016) but have presented evidence of dynamical metrics influencing retention. For instance, Simons et al. (2015) modeled two observed eddies in the California Current that had contrasting fish larval abundances; examination of the modeled eddies and tracked particles revealed high particle abundances for longer in the eddy rotating at a steady state in space and time, and low particle abundance or shorter retention in the eddy with unsteady rotation. In agreement, we find that water parcels inside a region of the eddy close to solid body rotation are likely to remain inside the eddy, while those outside are leaked more easily.

Similarly, Early et al. (2011) show that if the eddy rotational velocity exceeds translation velocity, there would be a region within the eddy that does not leak water; however, water loss may occur if the eddy decays. In agreement, we find that faster eddy rotation than translation is a necessary (but not sufficient)

condition for water to be retained by an eddy. Specifically, our results suggest that abrupt eddy changes, particularly toward elongation, are likely to allow water exchange with the surroundings. Changes in eddy shape may be caused by nonuniform vorticity and lead to loss of water from the eddy while undergoing geostrophic adjustment, or by instability and breakup of the vortex (de Steur & van Leeuwen, 2004). This mechanism has previously been associated with tracer filamentation and leakage due to differential rotation and eddy shape changes in Agulhas rings (de Steur & van Leeuwen, 2004).

4.4. Implications of Retention Times and Eddy Translation

4.4.1. Transport of Water Masses

Given the prevailing velocities at which eddies are advected, and usual retention times, mesoscale eddies have the potential to transport water across regions where water properties vary markedly. For instance, at a mean SW translation velocity of 0.3 m/s, median retention times of a month, and moving along a straight path, eddies could transport water from typical EAC separation latitudes (32°S) to 39°S just north of Tasmania; therefore, mesoscale eddies have the potential to move warm oligotrophic EAC waters into a region of colder waters of the Tasman Sea. Mean surface mixed layer temperatures in the Coral Sea (where the EAC forms) and the ocean off Tasmania differ by up to 12 °C (Condie & Dunn, 2006); thus, although eddies only contribute between 12.7% and 15.8% to the total poleward transport along the southeast coast of Australia (Cetina-Heredia et al., 2014) and that more than half the transport from the Tasman into the Indian Ocean occurs outside eddies (van Sebille et al., 2012), our results suggest the heat transport by these flow structures may not be negligible.

Assuming eddies are stationary and of constant volume, Rykova et al. (2017) estimated that anticyclonic eddies along southeastern Australia could contribute 8–46% of the heat entering the Tasman Sea. Similarly, to explore contemporary and future temperature transport by eddies along the EAC extension, Oliver et al. (2015) integrated the heat content of eddies by assuming that the zero contour of relative vorticity represented the radius within which tracer retention is high (Early et al., 2011). Oliver et al. (2015) found that eddies dominate the poleward transport of heat along the EAC extension south of 39°S. Our study shows that eddies along southeast Australia typically retain water parcels for a month while being advected; consequently, the assumptions of constant eddy volume or high retention are reasonable over this time period. Therefore, our results support the hypothesis that heat transport by eddies in the region is considerable. Other hydrographic properties may be modulated by eddies while advected due to water retention; Rykova and Oke (2015) found that cyclonic eddies have relatively low salinity; thus, freshening along the path of cyclonic eddies is a possible consequence. Furthermore, anticyclonic eddies formed during the summer season can retain large volumes of anomalously warm water in situ into the cooler winter season, which Chambers et al. (2015) showed contributed to damaging thunderstorm activity. Although water retention by eddies is key in their contribution to the transport of heat and other properties, ocean-atmosphere interactions including heat fluxes will also influence such process (e.g., Griffies et al., 2015).

4.4.2. Biogeochemical and Transport of Particulates

Anticyclonic eddies along the shelf break in southeast Australia are known to have considerably lower chlorophyll *a* concentrations than those in the Tasman Sea (Everett et al., 2015). In addition, we find that anticyclonic eddies moving along the shelf break generally have longer retention times than those offshore in the Tasman Sea (Figure 4); therefore, the along-shore transport of nutrient depleted waters by anticyclonic eddies is likely to be significant.

Eddies have been associated with a stepwise biogeochemical response consisting of nutrient injection and phytoplankton growth (Sweeney et al., 2003), which has been observed developing over short time periods of 2–5 days off California (Dugdale & Wilkerson, 1998) and over a month in the Sargasso Sea (McGillicuddy et al., 1998). Simons et al. (2015) emphasized that not only the lifespan of an eddy but whether they retain water plays an important role triggering this biogeochemical response. Retention times found in this study (median of approximately month) suggest that eddies along southeast Australia and in the Tasman Sea are likely to induce such cascading effect from nutrient supply to productivity.

Because eddies can induce productivity through upwelled nutrient enrichment, concentration, and retention (Bakun, 2006; Dufois et al., 2016), larval fish entrained in eddies can benefit from food availability throughout their development. The eddy retention times we find along southeast Australia not only are long enough for a phytoplankton response to nutrient rich waters but also affect phytoplankton species

interactions (Bracco et al., 2000; Perruche et al., 2011), attract organisms of higher trophic levels (e.g., Bakun, 2013; d'Ovidio et al., 2013), and influence connectivity patterns (Cetina-Heredia et al., 2019; Roughan et al., 2011) through the transport of larvae during their pelagic phase. We find mesoscale cyclonic eddies in the Tasman Sea move westward and potentially deliver water with higher nutrient concentrations and larvae into the continental shelf break, particularly at 32°S. This is in contrast to smaller frontal eddies that form on the inside edge of the EAC and translate offshore and poleward transporting shelf waters as observed by Roughan et al. (2017).

4.4.3. On Circulation Projections

Projections of circulation under a climate scenario show a larger proportion of anticyclones relative to cyclones relative to that of contemporary climate (from 20% to 70% more anticyclones than cyclones, Oliver et al., 2015) along southeast Australia. We find that typical retention times are similar irrespective of the direction of rotation; however, anticyclones have larger maximum retention time and often occur along the EAC extension, while cyclones are more spread across the Tasman Sea. As a consequence, a larger proportion of anticyclones in future scenarios would enhance poleward transport of water properties and larvae. In agreement, under the same climate scenario as that examined by Oliver et al. (2015), Cetina-Heredia et al. (2015) found that mesoscale eddy activity increases along the EAC extension inducing an increase in the amount of larvae reaching the coast between 36°S and 38°S relative to that in the contemporary scenario. Thus, the presence of even more anticyclones in future scenarios is likely to enhance heat transport and dispersal along the coast south of the EAC separation affecting heat distribution and changing connectivity patterns.

Acknowledgments

OFES data are available at http://apdrc.soest.hawaii.edu/; particle trajectories and associated spin parameter data are available at https://figshare.com/articles/particletraj_spin_mat/6977798; and MODIS and AVHRR satellite data were sourced from the Integrated Marine Observing System (IMOS, https://portal.aodn.org.au/). IMOS is supported by the Australian Government through the National Collaborative Research Infrastructure Strategy and the Super Science Initiative. P. C. H. was funded by ARC LP150100064 and DE130101336.

References

Abernathey, R., & Haller, G. (2018). Transport by Lagrangian vortices in the eastern Pacific. *Journal of Physical Oceanography*, *48*(3), 667–685. https://doi.org/10.1175/JPO-D-17-0102.1

Archer, M. R., Roughan, M., Keating, S. R., & Schaeffer, A. (2017). On the variability of the East Australian Current: Jet structure, meandering, and influence on shelf circulation. *Journal of Geophysical Research: Oceans*, *122*, 8464–8481. https://doi.org/10.1002/2017JC013097

Ardhuin, F., Aksenov, Y., Benetazzo, A., Bertino, L., Brandt, P., Caubet, E., et al. (2018). Measuring currents, ice drift, and waves from space: The Sea surface KInematics Multiscale monitoring (SKIM) concept. *Ocean Science*, *14*(3), 337–354. https://doi.org/10.5194/os-14-337-2018

Bakun, A. (2006). Fronts and eddies as key structures in the habitat of marine fish larvae: Opportunity, adaptive response and competitive advantage. *Scientia Marina*, *70*(S2), 105–122. https://doi.org/10.3989/scimar.2006.70s2105

Bakun, A. (2013). Ocean eddies, predator pits and bluefin tuna: Implications of an inferred 'low risk-limited payoff' reproductive scheme of a (former) archetypical top predator. *Fish and Fisheries*, *14*(3), 424–438. https://doi.org/10.1111/faf.12002

Benitez-Nelson, C. R., Bidigare, R. R., Dickey, T. D., Landry, M. R., Leonard, C. L., Brown, S. L., et al. (2007). Mesoscale eddies drive increased silica export in the subtropical Pacific Ocean. *Science*, *316*(5827), 1017–1021. https://doi.org/10.1126/science.1136221

Beron-Vera, F. J., Olascoaga, M. J., & Goni, G. J. (2008). Oceanic mesoscale eddies as revealed by Lagrangian coherent structures. *Geophysical Research Letters*, *35*, L12603. https://doi.org/10.1029/2008GL033957

Beron-Vera, F. J., Wang, Y., Olascoaga, M. J., Goni, G. J., & Haller, G. (2013). Objective detection of oceanic eddies and the Agulhas leakage. *Journal of Physical Oceanography*, *43*(7), 1426–1438. https://doi.org/10.1175/JPO-D-12-0171.1

Bracco, A., Provenzale, A., & Scheuring, I. (2000). Mesoscale vortices and the paradox of the plankton. *Proceedings of the Royal Society of London B*, *267*, 1795–1806.

Brach, L., Deixonne, P., Bernard, M.-F., Durand, E., Desjean, M.-C., Perez, E., et al. (2018). Anticyclonic eddies increase accumulation of microplastics in the North Atlantic subtropical gyre. *Marine Pollution Bulletin*, *126*, 191–196.

Brassington, G. B. (2010). Estimating surface divergence of ocean eddies using observed trajectories from a surface drifting buoy. *Journal of Atmospheric*, *27*(4), 705–720. https://doi.org/10.1175/2009JTECHO651.1

Brassington, G. B., Summons, N., & Lumpkin, R. (2011). Observed and simulated Lagrangian and eddy characteristics of the East Australian Current and the Tasman Sea. *Deep Sea Research*, *58*(5), 559–573. https://doi.org/10.1016/j.dsr2.2010.10.001

Bull, C., Kiss, A. E., Jourdain, N. C., England, M. H., & van Sebille, E. (2017). Wind forced variability in eddy formation, eddy shedding, and the separation of the East Australian Current. *Journal of Geophysical Research: Oceans*, *122*, 9980–9998. https://doi.org/10.1002/2017JC013311

Cetina-Heredia, P., Roughan, M., Liggins, G., Coleman, M. A., & Jeffs, A. (2019). Mesoscale circulation determines broad spatio-temporal settlement patterns of lobster. *PLoS ONE*, *14*(2), e0211722. https://doi.org/10.1371/journal.pone.0211722

Cetina-Heredia, P., Roughan, M., Sebille, E., Feng, M., & Coleman, M. A. (2015). Strengthened currents override the effect of warming on lobster larval dispersal and survival. *Global Change Biology*, *21*(12), 4377–4386. https://doi.org/10.1111/gcb.13063

Cetina-Heredia, P., Roughan, M., van Sebille, E., & Coleman, M. (2014). Long-term trends in the East Australian Current separation latitude and eddy driven transport. *Journal of Geophysical Research: Oceans*, *119*, 4351–4366. https://doi.org/10.1002/2014JC010071

Chaigneau, A., Gizolme, A., & Grados, C. (2008). Mesoscale eddies off Peru in altimeter records: Identification algorithms and eddy spatio-temporal patterns. *Progress in Oceanography*, *79*(2–4), 106–119. https://doi.org/10.1016/j.pocean.2008.10.013

Chambers, C. R. S., Brassington, G. B., Walsh, K., & Simmonds, I. (2015). Sensitivity of the distribution of thunderstorms to sea surface temperatures in four Australian east coast lows. *Meteorology and Atmospheric Physics*, *127*(5), 499–517. https://doi.org/10.1007/s00703-015-0382-4

Chelton, D. B., Gaube, P., Schlax, M. G., Early, J. J., & Samelson, R. M. (2011). The influence of nonlinear mesoscale eddies on near-surface oceanic chlorophyll. *Science*, *334*(6054), 328–332. https://doi.org/10.1126/science.1208897

Chelton, D. B., Schlax, M. G., & Samelson, R. M. (2011). Global observations of nonlinear mesoscale eddies. *Progress in Oceanography*, *91*(2), 167–216. https://doi.org/10.1016/j.pocean.2011.01.002

Chelton, D. B., Schlax, M. G., Samelson, R. M., & de Szoeke, R. A. (2007). Global observations of large oceanic eddies. *Geophysical Research Letters*, *34*, L15606. https://doi.org/10.1029/2007GL030812

Condie, S., & Condie, R. (2016). Retention of plankton within ocean eddies. *Global Ecology and Biogeography*, *25*(10), 1264–1277. https://doi.org/10.1111/geb.12485

Condie, S. A., & Dunn, J. R. (2006). Seasonal characteristics of the surface mixed layer in the Australasian region: Implications for primary production regimes and biogeography. *Marine and Freshwater Research*, *57*(6), 569–590. https://doi.org/10.1071/MF06009

de Ruijter, W. P. M., Biastoch, A., Drijfhout, S. S., Lutjeharms, J. R. E., Matano, R. P., Pichevin, T., et al. (1999). Indian-Atlantic interocean exchange: Dynamics, estimation and impact. *Journal of Geophysical Research*, *104*(C9), 20,885–20,910. https://doi.org/10.1029/1998JC900099

de Steur, L., & van Leeuwen, P. J. (2004). Tracer leakage from modeled Agulhas rings. *Journal of Physical Oceanography*, *34*, 1388–1399.

Dong, C., Lin, X., Liu, Y., Nencioli, F., Chao, Y., Guan, Y., et al. (2012). Three-dimensional oceanic eddy analysis in the Southern California Bight from a numerical product. *Journal of Geophysical Research*, *117*, C00H14. https://doi.org/10.1029/2011JC007354

d'Ovidio, F., De Monte, S., Della Penna, A., Cotte, C., & Guinet, C. (2013). Ecological implications of eddy retention in the open ocean: A Lagrangian approach. *Journal of Physics A: Mathematical and Theoretical*, *46*(25), 254,023–254,044. https://doi.org/10.1088/1751-8113/46/25/254023

Dufois, F., Hardman-Mountford, N. J., Greenwood, J., Richardson, A. J., Feng, M., & Matear, R. (2016). Anticyclonic eddies are more productive than cyclonic eddies in subtropical gyres because of winter mixing. *Science Advances*, *2*(5), e1600282. https://doi.org/10.1126/sciadv.1600282

Dugdale, R. C., & Wilkerson, F. P. (1998). Silicate regulation of new production in the equatorial Pacific upwelling. *Nature*, *391*(6664), 270–273. https://doi.org/10.1038/34630

Duncombe Rae, C. M. (1991). Agulhas retroflexion rings in the South Atlantic Ocean. *South African Journal of Marine Science*, *11*(1), 327–344. https://doi.org/10.2989/025776191784287574

Early, J. J., Samelson, R. M., & Chelton, D. B. (2011). The evolution and propagation of quasigeostrophic ocean eddies. *Journal of Physical Oceanography*, *41*(8), 1535–1555. https://doi.org/10.1175/2011JPO4601.1

Everett, J. D., Baird, M. E., Oke, P. R., & Suthers, I. M. (2012). An avenue of eddies: Quantifying the biophysical properties of mesoscale eddies in the Tasman Sea. *Geophysical Research Letters*, *39*, L16608. https://doi.org/10.1029/2012GL053091

Everett, J. D., Macdonald, H., Baird, M. E., Humphries, J., Roughan, M., & Suthers, I. (2015). Cyclonic entrainment of preconditioned shelf waters into a frontal eddy. *Journal of Geophysical Research: Oceans*, *120*, 677–691. https://doi.org/10.1002/2014JC010301

Falkowski, P. G., Ziemann, D., Kolber, Z., & Bienfang, P. K. (1991). Role of eddy pumping in enhancing primary production in the ocean. *Letters to Nature*, *352*(6330), 55–58. https://doi.org/10.1038/352055a0

Flierl, G. R. (1981). Particle motions in large-amplitude wave fields. *Geophysical and Astrophysical Fluid Dynamics*, *18*(1–2), 39–74. https://doi.org/10.1080/03091928108208773

Froyland, G., Horenkamp, C., Rossi, V., & van Sebille, E. (2015). Studying an Agulhas ring's long-term pathway and decay with finite-time coherent sets. *Chaos*, *25*(8), 083119. https://doi.org/10.1063/1.4927830

Griffa, A., Lumpkin, R., & Veneziani, M. (2008). Cyclonic and anticyclonic motion in the upper ocean. *Geophysical Research Letters*, *35*, L01608. https://doi.org/10.1029/2007GL032100

Griffies, S. M., & Treguier, A. M. (2013). *Ocean circulation models and modeling*, *International geophysics* (Vol. 103 pp. 521–551). Elsevier. https://doi.org/10.1016/B978-0-12-391851-2.00020-9

Griffies, S. M., Winton, M., Anderson, W. G., Benson, R., Delworth, T. L., Dufour, C. O., et al. (2015). Impacts on ocean heat from transient mesoscale eddies in a hierarchy of climate models. *Journal of Climate*, *28*(3), 952–977. https://doi.org/10.1175/JCLI-D-14-00353.1

Haller, G. (2005). An objective definition of a vortex. *Journal of Fluid Mechanics*, *525*, 1–26. https://doi.org/10.1017/S0022112004002526

Haller, G., & Beron-Vera, F. J. (2013). Coherent Lagrangian vortices: The black holes of turbulence. *Journal of Fluid Mechanics*, *731*(R4). https://doi.org/10.1017/jfm.2013.391

Kerry, C., Powell, B., Roughan, M., & Oke, P. R. (2016). Development and evaluation of a high-resolution reanalysis of the East Australian Current using the Regional Ocean Modelling System (ROMS 3.4) and Incremental Strong-constraint 4-Dimensional Variational data assimilation (IS4D-Var). *Geoscientific Model Development*. https://doi.org/10.5194/gmd-2016-44

Lehahn, Y., d'Ovidio, F., Levy, M., & Heifetz, E. (2007). Stirring of the northeast Atlantic spring bloom: A Lagrangian analysis based on multisatellite data. *Journal of Geophysical Research*, *112*, C08005. https://doi.org/10.1029/2006JC003927

Lilly, J. M., Scott, R. K., & Olhede, S. C. (2011). Extracting waves and vortices from Lagrangian trajectories. *Geophysical Research Letters*, *38*, L23605. https://doi.org/10.1029/2011GL049727

Lin, X., Dong, C., Chen, D., Liu, Y., Yang, J., Zou, B., & Guan, Y. (2015). Three-dimensional properties of mesoscale eddies in the South China Sea based on eddy-resolving model output. *Deep Sea Research, Part I*, *99*, 46–64. https://doi.org/10.1016/j.dsr.2015.01.007

Lindo-Atichati, D., Bringas, F., & Goni, G. (2013). Loop current excursions and ring detachments during 1993–2009. *International Journal of Remote Sensing*, *34*(14), 5042–5053. https://doi.org/10.1080/01431161.2013.787504

Liu, Y., Dong, C., Guan, Y., Dake, C., McWilliams, J., & Nencioli, F. (2012). Eddy analysis in the subtropical zonal band of the North Pacific Ocean. *Deep Sea Research, Part I*, *68*, 54–67. https://doi.org/10.1016/j.dsr.2012.06.001

Macdonald, H., Roughan, M., Baird, M., & Wilkin, J. (2016). The formation of a cold-core eddy in the East Australian Current. *Continental Shelf Research*, *114*, 72–84. https://doi.org/10.1016/j.csr.2016.01.002

Mantovanelli, A., Keating, S., Wyatt, L. R., Roughan, M., & Schaeffer, A. (2017). Lagrangian and Eulerian characterization of two counterrotating submesoscale eddies in a western boundary current. *Journal of Geophysical Research: Oceans*, *122*, 4902–4921. https://doi.org/10.1002/2016JC011968

Masumoto, Y., Sasaki, H., Kagimoto, T., Komori, N., Ishida, A., Sasai, Y., et al. (2004). A fifty-year eddy-resolving simulation of the world ocean: Preliminary outcomes of OFES (OGCM for the Earth Simulator). *Journal of the Earth Simulator*, *1*, 35–56.

Mata, M., Wijffels, S. E., Church, J. A., & Tomczak, M. (2006). Eddy shedding and energy conversion in the East Australian Current. *Journal of Geophysical Research*, *111*, C09034. https://doi.org/10.1029/2006JC003592

Matear, R., Chamberlain, M., Sun, C., & Feng, M. (2013). Climate change projection of the Tasman Sea from an eddy-resolving ocean model. *Journal of Geophysical Research: Oceans*, *118*, 2961–2976. https://doi.org/10.1002/jgrc.20202

McGillicuddy, D. J. Jr., Robinson, A. R., Siegel, D. A., Jannasch, H. W., Johnson, R., Dickey, T. D., et al. (1998). Influence of mesoscale eddies on new production in the Sargasso Sea. *Letters to Nature*, *394*(6690), 263–266. https://doi.org/10.1038/28367

Nencioli, F., Dong, C., Dickey, T., Washburn, L., & McWilliams, J. (2010). A vector geometry based eddy detection algorithm and its application to high-resolution numerical model products and high-frequency radar surface velocities in the Southern California Bight. *Journal of Atmospheric and Oceanic Technology*, *27*, 564–579. https://doi.org/10.1175/2009JTECHO725.1

O'Kane, T., Oke, P. R., & Sandery, P. A. (2011). Predicting the East Australian Current. *Ocean Modelling*, *38*(3-4), 251–266. https://doi.org/10.1016/j.ocemod.2011.04.003

Oke, P. R., & Griffin, D. A. (2011). The cold-core eddy and strong upwelling off the coast of New South Wales in early 2007. *Deep Sea Research*, *58*(5), 574–591.

Oliver, E. C. J., O'Kane, T. J., & Holbrook, N. (2015). Projected changes to Tasman Sea eddies in a future climate. *Journal of Geophysical Research: Oceans*, *120*, 7150–7165. https://doi.org/10.1002/2015JC010993

Paris, C. B., Helgers, H., van Sebille, E., & Srinivasan, A. (2013). The Connectivity Modelling System: A probabilistic tool for the multi-scale tracking of biotic and abiotic variability in the ocean. *Environmental Modelling and Software*, *42*, 47–54. https://doi.org/10.1016/j.envsoft.2012.12.006

Perruche, C., Riviere, P., Lapeyre, G., Carton, X., & Pondaven, P. (2011). Effects of surface quasi-geostrophic turbulence on phytoplankton competition and coexistence. *Journal of Marine Research*, *69*(1), 105–135. https://doi.org/10.1357/002224011798147606

Pilo, G. S., Mata, M. M., & Azevedo, J. L. L. (2015). Eddy surface properties and propagation at Southern Hemisphere western boundary current systems. *Ocean Science*, *11*(4), 629–641. https://doi.org/10.5194/os-11-629-2015

Pilo, G. S., Oke, P. R., Coleman, R., Rykova, T., & Ridgway, K. (2018). Patterns of vertical velocity induced by eddy distortion in an ocean model. *Journal of Geophysical Research: Oceans*, *123*, 2274–2292. https://doi.org/10.1002/2017JC013298

Pilo, G. S., Oke, P. R., Rykova, T., Coleman, R., & Ridgway, K. (2015). Do East Australian Current anticyclonic eddies leave the Tasman Sea? *Journal of Geophysical Research: Oceans*, *120*, 8099–8114. https://doi.org/10.1002/2015JC011026

Qiu-Yang, L., Sun, L., & Sheng-Fu, L. (2016). GEM: Dynamic tracking model for mesoscale eddies in the ocean. *Ocean Science*, *12*(6), 1249–1267. https://doi.org/10.5194/os-12-1249-2016

Ridgway, K. R., & Dunn, J. R. (2003). Mesoscale structure of the mean East Australian Current system and its relationship with topography. *Progress in Oceanography*, *56*(2), 189–222. https://doi.org/10.1016/S0079-6611(03)00004-1

Roughan, M., Keating, S., Schaeffer, A., Cetina Heredia, P., Rocha, C., Griffin, D., et al. (2017). A tale of two eddies: The biophysical characteristics of two contrasting cyclonic eddies in the East Australian Current System. *Journal of Geophysical Research: Oceans*, *122*, 2494–2518. https://doi.org/10.1002/2016JC012241

Roughan, M., Macdonald, H. S., Baird, M. E., & Glasby, T. M. (2011). Modelling coastal connectivity in a western boundary current: Seasonal and inter-annual variability. *Deep Sea Research, Part II*, *58*(5), 628–644. https://doi.org/10.1016/j.dsr2.2010.06.004

Rykova, T., & Oke, P. R. (2015). Recent freshening of the East Australian Current and its eddies. *Geophysical Research Letters*, *42*, 9369–9378. https://doi.org/10.1002/2015GL066050

Rykova, T., Oke, P. R., & Griffin, D. A. (2017). A comparison of the structure, properties, and water mass composition of quasi-isotropic eddies in western boundary currents in an eddy-resolving ocean model. *Ocean Modelling*, *114*, 1–13. https://doi.org/10.1016/j.ocemod.2017.03.013

Sadarjoen, A., Post, F. H., Bing, M., Banks, D. C., & Pagendarm, H.-G. (1998). Selective visualization of vortices in hydrodynamic flows. In *Proceedings of visualization '98* (pp. 419–422). NC: Research Triangle Park.

Schaeffer, A., Gramoulle, A., Roughan, M., & Mantovanelli, A. (2017). Characterizing frontal eddies along the East Australian Current from HF radar observations. *Journal of Geophysical Research: Oceans*, *122*, 3964–3980. https://doi.org/10.1002/2016JC012171

Schiller, A., Oke, P. R., Brassington, G. B., Entel, M., Fiedler, R., Griffin, D. A., & Mansbridge, J. V. (2008). Eddy-resolving ocean circulation in the Asian-Australian region inferred from an ocean reanalysis effort. *Progress in Oceanography*, *76*(3), 334–365. https://doi.org/10.1016/j.pocean.2008.01.003

Simons, R. D., Nishimoto, M. M., Washburn, L., Brown, K. S., & Siegel, D. A. (2015). Linking kinematic characteristics and high concentrations of small pelagic fish in a coastal mesoscale eddy. *Deep Sea Research, Part I*, *100*, 34–47. https://doi.org/10.1016/j.dsr.2015.02.002

Sweeney, E., McGillicuddy, D., & Buesseler, K. (2003). Biogeochemical impacts due to mesoscale eddy activity in the Sargasso Sea as measured in the Bermuda Atlantic Time-Series Study (BATS). *Deep-Sea Research Part II*, *50*(22-26), 3017–3039. https://doi.org/10.1016/j.dsr2.2003.07.008

The Ring Group (1981). Gulf Stream cold-core rings: Their physical, chemistry and biology. *Science*, *212*(4499), 1091–1100. https://doi.org/10.1126/science.212.4499.1091

van Sebille, E., England, M. H., Zika, J. D., & Sloyan, B. (2012). Tasman leakage in a fine-resolution ocean model. *Geophysical Research Letters*, *39*, L06601. https://doi.org/10.1029/2012GL051004

Veneziani, M., Griffa, A., Garraffo, Z. D., & Chassignet, E. P. (2005). Lagrangian spin parameter and coherent structures from trajectories released in a high-resolution ocean model. *Journal of Marine Research*, *63*(4), 753–788. https://doi.org/10.1357/0022240054663187

Veneziani, M., Griffa, A., Reynolds, A. M., Garraffo, Z. D., & Chassignet, E. P. (2005). Parameterization of Lagrangian spin statistics and particle dispersion in the presence of coherent vortices. *Journal of Marine Research*, *63*(6), 1057–1083. https://doi.org/10.1357/002224005775247571

Veneziani, M., Griffa, A., Reynolds, A. M., & Mariano, A. J. (2004). Oceanic turbulent and stochastic models from subsurface Lagrangian data for the northwest Atlantic Ocean. *Journal of Physical Oceanography*, *34*(8), 1884–1906. https://doi.org/10.1175/1520-0485(2004)034<1884:OTASMF>2.0.CO;2

Wang, Y., Olascoaga, M. J., & Beron-Vera, F. J. (2015). Coherent water transport across the South Atlantic. *Geophysical Research Letters*, *42*, 4072–4079. https://doi.org/10.1002/2015GL064089

Yeung, C., Jones, D. L., Criales, M. M., Jackson, T., & Richards, W. J. (2001). Influence of coastal eddies and counter-currents on the influx of spiny lobster, Panulirus argus, postlarvae into Florida Bay. *Marine and Freshwater Research*, *52*(8), 1217–1232. https://doi.org/10.1071/MF01110

Zhang, Z., Wang, W., & Qiu, B. (2014). Oceanic mass transport by mesoscale eddies. *Science*, *345*(6194), 322–324. https://doi.org/10.1126/science.1252418